Glucose and SIRT2 reciprocally mediate the regulation of keratin 8 by lysine acetylation

Natasha T. Snider,[1] Jessica M. Leonard,[1] Raymond Kwan,[1] Nicholas W. Griggs,[1] Liangyou Rui,[1] and M. Bishr Omary[1,2]

[1]Department of Molecular and Integrative Physiology and [2]Department of Medicine, University of Michigan Medical School, Ann Arbor, MI 48109

Lysine acetylation is an important posttranslational modification that regulates microtubules and microfilaments, but its effects on intermediate filament proteins (IFs) are unknown. We investigated the regulation of keratin 8 (K8), a type II simple epithelial IF, by lysine acetylation. K8 was basally acetylated and the highly conserved Lys-207 was a major acetylation site. K8 acetylation regulated filament organization and decreased keratin solubility. Acetylation of K8 was rapidly responsive to changes in glucose levels and was up-regulated in response to nicotinamide adenine dinucleotide (NAD) depletion and in diabetic mouse and human livers. The NAD-dependent deacetylase sirtuin 2 (SIRT2) associated with and deacetylated K8. Pharmacologic or genetic inhibition of SIRT2 decreased K8 solubility and affected filament organization. Inhibition of K8 Lys-207 acetylation resulted in site-specific phosphorylation changes of K8. Therefore, K8 acetylation at Lys-207, a highly conserved residue among type II keratins and other IFs, is up-regulated upon hyperglycemia and down-regulated by SIRT2. Keratin acetylation provides a new mechanism to regulate keratin filaments, possibly via modulating keratin phosphorylation.

Introduction

Protein lysine acetylation is a reversible process involving the modification of ε-amino groups of lysine residues with an acetyl moiety from acetyl-CoA (Yang and Seto, 2008; Kim and Yang, 2011). The dynamics of this process are regulated by specific enzymes carrying out lysine acetylation and deacetylation in response to different stimuli (Aka et al., 2011). For example, acetylation has a major role regulating metabolism, as most metabolic enzymes are acetylated in response to the type and abundance of cellular energy source (Zhao et al., 2010). Further, a global proteome analysis identified acetylation as a highly pervasive modification able to alter functional protein networks, thereby modulating cell cycle regulation, DNA repair, nuclear transport, and cytoskeletal dynamics (Choudhary et al., 2009).

Although microtubule cytoskeletal dynamics have long been known to be regulated by the reversible acetylation of α-tubulin at Lys-40 (L'Hernault and Rosenbaum, 1985), the exact functional significance of this process is unclear. However, α-tubulin acetylation is associated with microtubule stabilization (Janke and Bulinski, 2011). Similarly, actin is acetylated at Lys-61 and its acetylation is linked to the formation of stabilized actin stress fibers (Kim et al., 2006). In stark contrast, there is lack of insight into the extent to which lysine acetylation plays a role in the function of intermediate filament proteins (IFs). A better understanding of IF regulation by acetylation should provide important insight into the role of acetylation on cytoskeletal dynamics in general.

The IF cytoskeleton of simple-type epithelia consists of heteropolymers between keratin 8 (K8) and K18. Mutations in human K8 (e.g., G62C and R341H) predispose their carriers to acute and chronic liver disease progression (Omary et al., 2009; Strnad et al., 2010). A properly functioning IF cytoskeleton is critical for the ability of cells to cope with stress (Toivola et al., 2010). Stress-mediated posttranslational modifications in normal and diseased human liver, including phosphorylation (Omary et al., 2006), transamidation (Kwan et al., 2012), sumoylation (Snider et al., 2011), and their cross talk, have important consequences on keratin filament organization. Recent proteomic studies revealed multiple potential acetylated sites on K8 and K18 (Leech et al., 2008; Choudhary

Correspondence to Natasha Snider: nsnider@umich.edu

Abbreviations used in this paper: AcK, acetyl-lysine; AU, acid urea; HMM, high molecular mass; HSE, high salt extract; IF, intermediate filament protein; K8, keratin 8; SIRT2, sirtuin 2; WT, wild type.

The Rockefeller University Press $30.00
J. Cell Biol. Vol. 200 No. 3 241–247
www.jcb.org/cgi/doi/10.1083/jcb.201209028

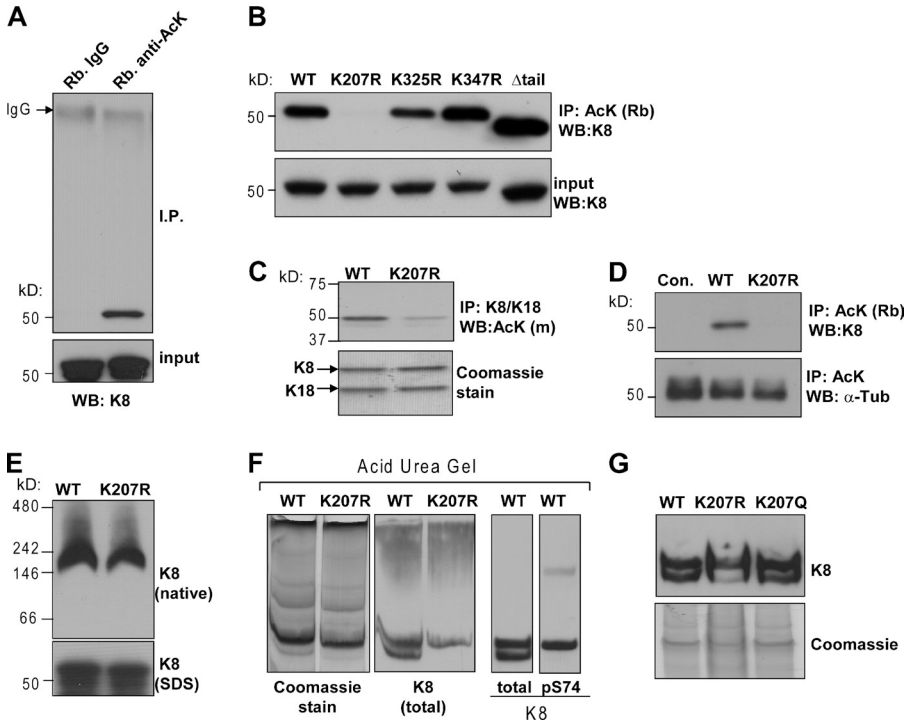

Figure 1. **Human K8 is basally acetylated at the highly conserved Lys-207.** (A) K8 is basally acetylated in HT29 cells, as demonstrated by immunoprecipitation using rabbit anti-acetylated lysine (AcK) antibody and K8 immunoblot. (B) Comparison of acetylation status of WT human K8, three Lys-to-Arg mutants, and a C-terminal deletion mutant lacking Lys-472 and Lys-483. BHK-21 cells were transfected with constructs expressing the designated K8 variant together with WT K18, followed by lysis and immunoprecipitation of acetylated proteins using a rabbit anti-AcK antibody and K8 immunoblot. (C) K8/K18 immunoprecipitation from lysates of BHK-21 cells expressing either WT or K207R K8, followed by immunoblot with a mouse (m) anti-AcK antibody. (D) BHK-21 cells that were untransfected (Con.) or transfected with WT or K207R K8 were lysed followed by rabbit anti-AcK immunoprecipitation and K8 or α-tubulin immunoblotting. (E) Native gel electrophoresis of WT and K207R K8 showing that the mutation does not affect K8/K18 tetramer formation. (F and G) Analysis of WT, K207R, and K207Q K8 by AU gel electrophoresis followed by Coomassie staining and immune blotting for total or phospho-K8 (pS74).

et al., 2009), but these sites have yet to be validated and their significance investigated. The goals of the present study were to investigate the regulation of K8 by lysine acetylation and identify the specific sites, contexts, and consequences associated with this modification.

Results and discussion

Identification of Lys-207 as a major acetylation site on human K8

Using high-resolution mass spectrometry, Choudhary et al. (2009) identified 1,750 acetylated proteins with 3,600 corresponding lysine acetylation sites. K8 was among the proteins identified by this method and found to have five acetylation sites (Lys-117, Lys-207, Lys-295, Lys-325, and Lys-347), all located within the coiled-coil rod domain region of the protein (Herrmann et al., 2009). Evidence that lysines located outside of the rod domain may also be subject to acetylation came from another proteomic study that identified Lys-472 and Lys-483 in the tail domain of K8 as being acetylated (Leech et al., 2008). The aforementioned studies used human cell lines of lymphoid (MV4-11 and Jurkat) or epithelial (A549 and HCT116) origin. To determine if these data can be validated in normal tissue, we performed mass spectrometry analysis on human K8 derived from livers of human K8-overexpressing mice (Nakamichi et al., 2005). Three of the seven lysines identified by prior proteomic studies were acetylated in normal liver under basal conditions, i.e., in the absence of injury or deacetylase inhibitors (Fig. S1 A). We also detected basal K8 acetylation in human colon carcinoma HT29 cells, as determined by immune isolation using a rabbit anti-acetyl-lysine (anti-AcK) antibody followed by blotting with anti-K8 antibody (Fig. 1 A).

We next performed site-directed mutagenesis (Lys-to-Arg) or used a C-terminal truncated version of K8 lacking the last 14 amino acids, including Lys-472 and Lys-483 (Ku et al., 2005), to determine which K8 residues are major acetylation sites. Relative to wild-type (WT) K8, the acetylation of the K207R mutant was negligible, suggesting that Lys-207 is a major acetylation site (Fig. 1 B). Acetylated K8 is also detected after K8/K18 immunoprecipitation, followed by blotting with a mouse anti-AcK antibody (Fig. 1 C). The effect of the mutation was not a result of a general acetylation defect because acetylation of α-tubulin was unaltered (Fig. 1 D). As an additional control, we tested whether the K207R mutation affects K8/K18 tetramer formation and found that it was not the case (Fig. 1 E). To assess K8 acetylation independently of the AcK antibody method, we examined K8 migration by acid urea (AU) gel electrophoresis. Because urea leads to protein denaturation without altering the charge, the migration profile of proteins is determined by the number of protonated groups, as shown for histone acetylation (Shechter et al., 2007). Notably, two distinct bands for the WT K8 protein but only one for the K207R mutant are resolved (Fig. 1 F). Because the phosphorylated form of K8 comigrates with the top band (Fig. 1 F), we conclude that the second band, lacking in the K207R mutant, most likely contains acetylated K8. Importantly, the K8 band lacking in the Lys-207 arginine mutant is restored when Lys-207 is mutated to an acetyl-mimetic glutamine (Fig. 1 G).

K8 acetylation is important for filament organization and solubility

Given that Lys-207 is highly conserved (Fig. S1 B), we hypothesized that its acetylation status may regulate K8/K18 filament properties. Therefore, we compared the filament organization of

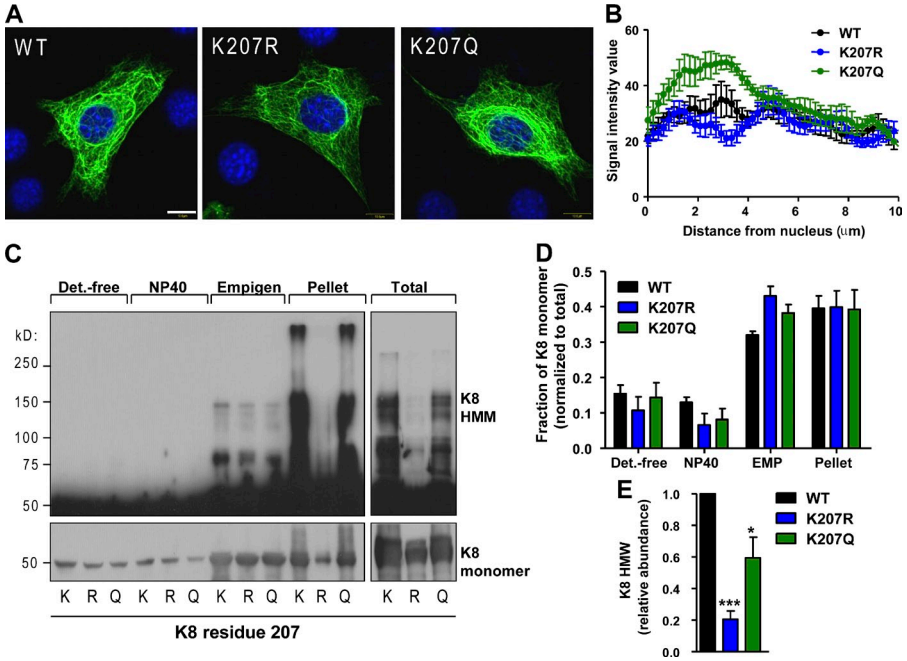

Figure 2. **K8 acetylation affects keratin filament organization and solubility properties.** (A) Representative images from NIH-3T3 cells expressing WT, K207R, and K207Q K8. Bar, 10 µm. (B) Quantification of the K8 signal intensity as a function of distance from the cell nucleus (n = 5). (C) Western blot analysis under reducing conditions of WT, K207R, and K207Q-K8 from sequential subcellular fractions (long and short exposures of the same membrane are shown at the top and bottom, respectively). (D) Quantification of the K8 monomer band from three separate experiments. (E) Quantification of the K8 HMM signal from three separate experiments. ***, $P < 0.001$; *, $P < 0.05$; relative to WT; one-way analysis of variance. The results are presented as the mean and the standard deviation.

WT K8 with the acetylation-deficient K207R and acetylation-mimetic K207Q mutants. We observed differences in filament density surrounding the nuclei (Fig. 2 A) and quantitative analysis of the image data (Fig. S2, A and B) showed an increase in the signal intensity for K207Q and a decrease for K207R within a distance of ∼2–4 µm from the nuclei relative to WT K8 (Fig. 2 B). We next assessed the effect of these mutations on K8 solubility by a sequential fractionation method using a detergent-free buffer, followed by nonionic (NP-40) and ionic (Empigen) detergent solubilization and compared these fractions to the remaining pellet and total K8 by immune blotting (Fig. 2 C). There was no significant difference between the amounts of K8 monomer in each fraction relative to total K8 (Fig. 2 D). However, one major difference was in the presence of high molecular mass (HMM) K8 species in the insoluble pellet. Compared with WT K8, the abundance of these K8 complexes, which we observed under reducing and nonreducing (not depicted) conditions, was diminished by 80% in the K207R mutant and partially restored in the K207Q mutant (Fig. 2 E). This was confirmed using two independent K8 antibodies (Fig. S1 C). These findings indicate that acetylation regulates K8 filament organization and solubility properties.

K8 acetylation is regulated by glucose concentration in vitro and in vivo

Because acetyl-CoA is a donor of the acetyl group in lysine acetylation reactions, we investigated the dynamics of K8 acetylation in response to glucose availability. As shown in Fig. 3 A, K8 acetylation at Lys-207 is minimal after transient (6-h) glucose deprivation, but is rapidly (within 1 h) and dose dependently increased in response to glucose addition. To confirm that this occurs in normal tissues, we investigated mouse K8 acetylation in vivo under normoglycemic and hyperglycemic conditions by comparing livers from WT and ob/ob (leptin-deficient) mice. Basal mouse liver K8 acetylation was up-regulated in the setting of hyperglycemia (Fig. 3 B and Fig. S3 A), whereas α-tubulin acetylation was unchanged (Fig. 3 B). Further, K8 acetylation in diabetic human liver tissue was also dramatically increased (Fig. 3 C). Thus, K8 acetylation is dynamically regulated in response to physiological and pathological alterations in glucose concentration.

Sirtuin 2 (SIRT2) functions as a K8 deacetylase

Nutrient availability also impacts acetylation reactions via modulating the activity of sirtuins, energy-sensitive NAD-dependent deacetylases (Schwer and Verdin, 2008; Imai and Guarente, 2010). Treatment of cells with FK866, an NAD synthesis inhibitor (Hasmann and Schemainda, 2003), significantly augmented K8 acetylation (Fig. 3 D). There are seven mammalian sirtuins (SIRT1–7), but only SIRT1–3 and SIRT7 have deacetylase activity (Imai and Guarente, 2010). SIRT2 is the only isoform found primarily in the cytosol. Coimmunoprecipitation revealed an interaction between SIRT2 and K8 under glucose-free and low glucose conditions, which was diminished in the presence of high glucose (Fig. 3 E). Intracellular cross-linking revealed the existence of an ∼90-kD protein complex (Fig. 3 F), corresponding to the combined molecular sizes of K8 and SIRT2, which is consistent with a direct association. Further, upon overexpressing SIRT1 or SIRT2, we detected a significant amount of SIRT2, but not SIRT1, present in the keratin-rich insoluble high salt extract (HSE), as seen by both immunoblot and Coomassie (Fig. 3 G). The partitioning of SIRT2 into the HSE is directly dependent on the amount of K8/K18 expressed (Fig. 3 H). SIRT2 levels and K8/K18 filament organization do not differ between WT and ob/ob mice (Fig. S3, B and C). In contrast, we found decreased SIRT2 expression in cirrhotic human liver explants, which was associated with an increase in K8 acetylation (Fig. S3 D).

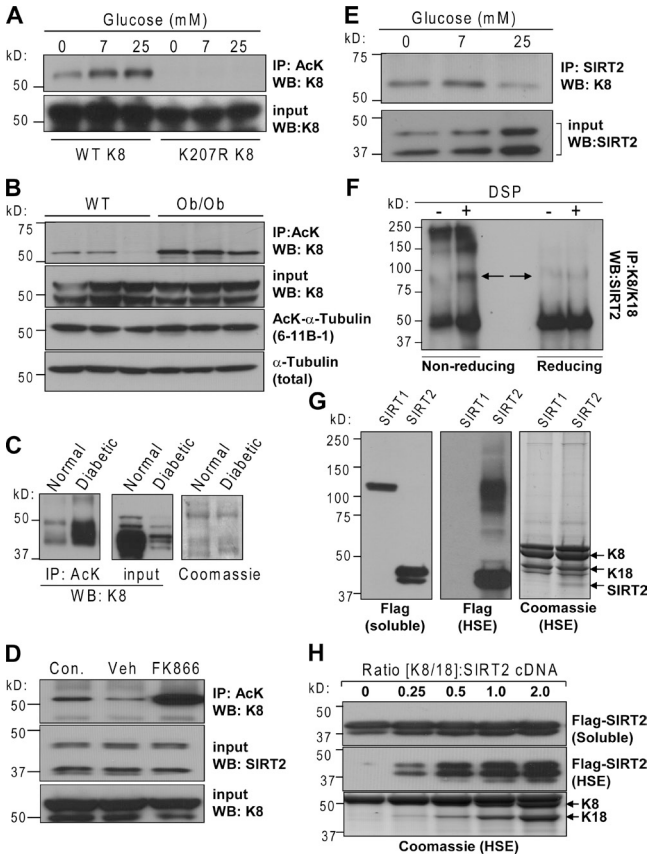

Figure 3. **K8 acetylation is dynamically up-regulated by glucose in vitro and in vivo.** (A) BHK-21 cells expressing WT or K207R K8 were cultured in glucose-free medium for 6 h followed by 1-h incubation in glucose-free (0 mM), low (7 mM), or high (25 mM) glucose medium. The cell lysates were immunoprecipitated with a rabbit anti-AcK antibody followed by K8 immunoblotting. (B) Liver lysates from three individual WT or ob/ob mice (see Materials and methods) were immunoprecipitated with rabbit AcK antibody followed by immunoblotting for K8. Total and acetylated α-tubulin blots were done for comparison. (C) K8 acetylation in normal and diabetic human liver tissue. (D) K8 acetylation in control, vehicle-, and FK866-treated (NAD-depleted) cells. Two isoforms of SIRT2 protein migrate at 37 and 43 kD. (E) Immunoprecipitation using rabbit anti-SIRT2 antibody from lysates of HepG2 cells cultured under different glucose conditions followed by K8 immunoblotting demonstrates a glucose-sensitive K8–SIRT2 interaction. (F) Glucose-starved (3 h) HepG2 cells were incubated in the absence (–) or presence (+) of the cell-permeable cross-linker DSP and lysed, and the K8/K18 immunoprecipitates were analyzed by blotting for SIRT2 under nonreducing or reducing conditions. Arrows highlight the 90-kD species. (G) Flag-tagged human SIRT1 or SIRT2 were coexpressed with WT K8/K18 in BHK-21 cells and the Triton X-100 (soluble) and HSE fractions were analyzed by Flag immunoblot or Coomassie stain. (H) Same as G, except that different amounts of K8/K18 cDNA were cotransfected.

Alteration of keratin acetylation, solubility, and filament organization in response to changes in SIRT2 levels and activity

Upon overexpression, SIRT2 displayed a cytoplasmic distribution and colocalized with endogenous K8 (Fig. 4 A). The multinucleation is consistent with the known role of SIRT2 in regulating mitotic exit and genome integrity (Dryden et al., 2003; Kim et al., 2011). Overexpression of SIRT2 significantly decreased acetylated K8 (Fig. 4 B), whereas increased K8 acetylation was detected after SIRT2 knockdown (Fig. 4 C and Fig. S3 E). Use of the SIRT2-selective inhibitor AGK2 (Outeiro et al., 2007) further demonstrated that SIRT2 is involved in K8 deacetylation under both glucose-deficient and -replete conditions (Fig. 4 D). AGK2 caused a dose-dependent decrease in soluble K8 (Fig. 4 E) and formation of HMM K8/K18 complexes (Fig. 4 F and Fig. S3 F) and increased K8/K18 acetylation (Fig. 4 F). There was a general filament reorganization and an appearance of perinuclear K8/K18 aggregates in ∼5–10% of the cells treated with AGK2 (Fig. 4 G). These data indicate a functional connection between SIRT2 and K8 deacetylation with significant consequences to filament organization.

Acetylation modulates K8 site-specific phosphorylation

K8 serine phosphorylation is known to promote solubility (Omary et al., 1998, 2006), whereas we show here that acetylation decreases K8 solubility. Therefore, we investigated a potential effect of K8 acetylation on K8 phosphorylation. As shown in Fig. 5 (A and B), K8 Ser-74 (but not Ser-432) phosphorylation is significantly diminished in the K207R mutant and restored to near baseline WT levels in the K207Q acetylation mimetic. These data suggest that acetylation of K8 at Lys-207 may exert some of its effects on keratin filament organization by modulation of site-specific K8 phosphorylation. This is supported by prior evidence showing that phosphorylation of K8 at Ser-74 plays an important role in the ability of keratin filaments to reorganize (Ku et al., 2002). To that end, glucose starvation followed by restimulation leads to reorganization of K8/K18 filaments and appearance of strong perinuclear K8/K18 staining in association with increased K8 Ser-74 phosphorylation (Fig. 5 C).

In the present study we demonstrated a functional link between cellular metabolic status and site-specific K8 acetylation, with Lys-207 being a major site. The highly conserved nature of Lys-207 in K8 suggests that lysine acetylation may be an evolutionarily conserved process important for the regulation of other IFs. The sequence context of K8 Lys-207 (K-V/A-D/E-L-E) is also conserved among the type II keratins. We show that acetylation regulates perinuclear keratin filament organization (Fig. 2). Acetylation also promotes the formation of insoluble tightly associated K8 complexes, which may indicate a similarity to its role in promoting microtubule and microfilament stabilization (Kim et al., 2006; Janke and Bulinski, 2011). Although the mechanism of how K8 acetylation modulates keratin filament organization remains to be explored, the dramatic and site-specific effect of K8 Lys-207 acetylation on K8 Ser-74 phosphorylation (Fig. 5) suggests that modulation of keratin phosphorylation and possibly other posttranslational modifications could mediate such effects.

The increased K8 acetylation in diabetic animals may have important pathophysiological consequences during liver injury associated with the metabolic syndrome. SIRT2 levels are significantly diminished in adipose tissue from obese subjects and SIRT2 is transcriptionally repressed in diet-induced obesity (Krishnan et al., 2012). Collectively, our findings show that K8 Lys-207 is a highly conserved and dynamically acetylated residue that is targeted by SIRT2 and serves as a sensor of the cellular metabolic environment. This sensor effect could

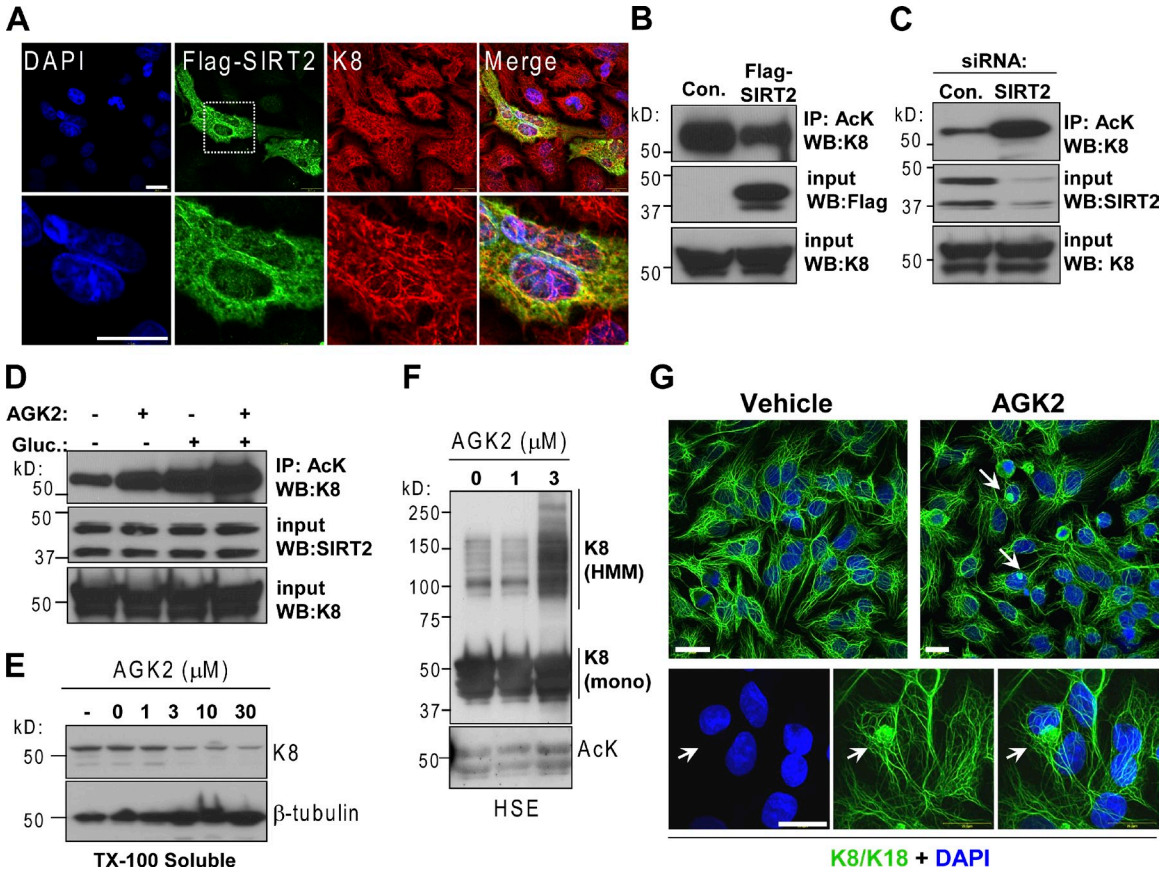

Figure 4. **K8 acetylation is dependent on SIRT2 activity and expression levels.** (A) Immunofluorescence staining of K8/K18 and Flag-SIRT2 in HepG2 cells shows significant colocalization. Bars, 20 µm. (B) Rabbit anti-AcK immunoprecipitation of untransfected and Flag-SIRT2–transfected HT29 cell lysates followed by K8 immunoblotting. (C) HT29 cells were transfected with control or SIRT2 siRNA for 18 h, followed by 6-h incubation in glucose-free medium. The lysates were analyzed by rabbit anti-AcK immunoprecipitation followed by K8 immunoblotting. (D) HT29 cells were cultured in the absence or presence of 25 mM glucose and 10 µM AGK2 for 6 h. The lysates were immunoprecipitated with rabbit anti-AcK antibody followed by K8 immunoblot. (E) HepG2 cells were untreated (−) or treated with DMSO vehicle (0) or different concentrations of AGK2 for 18 h and the Triton X-100–soluble fractions were assessed for the presence of K8 and β-tubulin (soluble fraction marker). (F) Immunoblot of K8 and AcK in HSEs of HT29 cells after treatment with vehicle (0) or AGK2 for 18 h. (G) Filament reorganization and perinuclear aggregate formation (arrows) in HepG2 cells treated with 10 µM AGK2 for 18 h. Bars, 20 µm.

provide a critical link in the chain of cellular events surrounding K8/K18-mediated protection during metabolic stress in hepatocytes (Loranger et al., 1997; Toivola et al., 2010) by, for example, linking nutrient availability to K8 phosphorylation.

Materials and methods

Antibodies and chemicals

The antibodies used in the study were rabbit anti-AcK (Abcam) and mouse anti-AcK Ac-K-103 (Cell Signaling Technology). Other antibodies were directed to acetylated α-tubulin (6-11B-1; Abcam); SIRT2 (EP1668Y; Epitomics); Flag (OriGene); β-tubulin, human K18 (DC10), and human K8 (mouse TS1 and rabbit EP1628Y [Thermo Fisher Scientific]); mouse K8 (Troma I; Developmental Studies Hybridoma Bank); K8 pSer74 (Liao et al., 1997); and K8 pS432 (Ku and Omary, 1997). The chemicals used were AGK2 (Tocris), dithiobis[succinimidylpropionate] (DSP; Thermo Fisher Scientific), and FK866 (Cayman Chemical).

Site-directed mutagenesis

The human K8 cDNA in vector pcDNA3.1 was mutated to generate single-point lysine to arginine or glutamine mutations using the QuikChange site-directed mutagenesis kit (Agilent Technologies). Generation of the truncated mutant of K8 was performed as described previously (Ku et al., 2005). In brief, a frame-shift mutation at Ile465 (ATC→ATCC) generates a truncated 468–amino acid protein (instead of 482). The WT and mutant keratin constructs were confirmed by DNA sequencing.

Cell cultures and transfection

BHK-21 (baby hamster kidney), NIH3T3 (mouse fibroblast), HepG2 (human hepatoma), and HT29 (human colon carcinoma) cells were obtained from American Type Culture Collection and maintained as recommended by the supplier. Lipofectamine 2000 (for BHK-21) or Lipofectamine LTX (for NIH3T3, HepG2, and HT29; Invitrogen) were used for transfections. Control and SIRT2 siRNA were obtained from Thermo Fisher Scientific and transfected into HT29 or HepG2 cells using RNAiMAX (Invitrogen) per the manufacturer's instructions. Plasmid encoding flag-tagged SIRT1 was provided by M. Greenberg (Harvard Medical School, Boston, MA) via Addgene (plasmid 1791) and SIRT2 plasmid was provided by E. Verdin (University of California, San Francisco, San Francisco, CA) via Addgene (plasmid 13813). Biochemical and immunofluorescence staining analyses were performed 18–48 h posttransfection.

Preparation of cell and tissue lysates, immunoprecipitation, and immunoblotting

Cultured cells or liver tissues were homogenized in ice-cold NP-40 buffer (150 mM sodium chloride, 1% NP-40, and 50 mM Tris, pH 8.0) supplemented with protease inhibitors. Immunoprecipitation was performed using antibodies to AcK or K8/K18 (DC10 or TS1) conjugated to Dynabeads–Protein G (Invitrogen) for 2–3h at 4°C with shaking. To induce intracellular cross-linking before cell lysis, the cell-permeable cross-linker DSP was added to HepG2 cells for 30 min at room temperature following manufacturer recommendations. 2-Mercaptoethanol was added to some samples to reverse cross-linking before analysis. To induce NAD depletion, cells were treated with 10 nM FK866 for 18 h. Total lysates and immunoprecipitates were resolved on gradient 4–20% or 10% SDS-PAGE gels and were transferred onto polyvinylidene difluoride membranes, which were then blocked

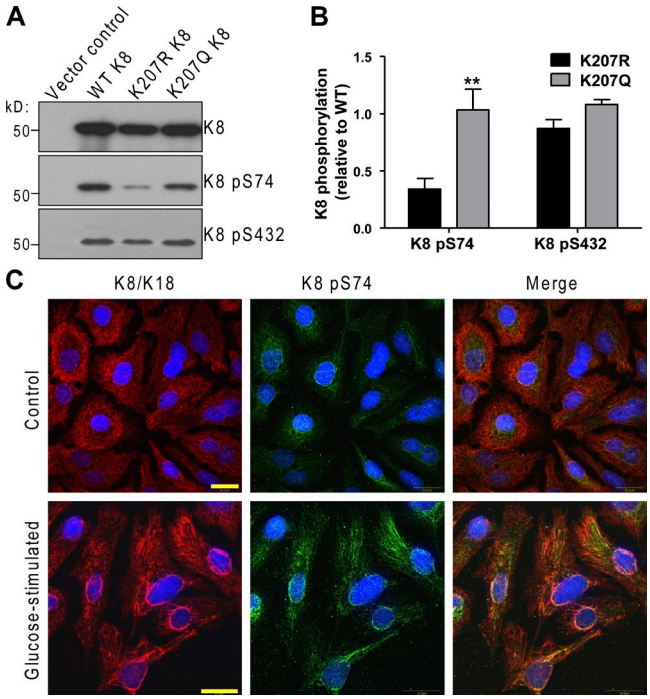

Figure 5. **Acetylation and glucose stimulation modulate K8 site-specific phosphorylation.** (A) BHK-21 cells were transfected with the indicated plasmids followed by analysis of the total cell lysates by immunoblotting for total and phospho-K8 (pS74 and pS432). (B) Quantification of the immunoblot data shown in A from three separate experiments. **, $P < 0.01$; one-way analysis of variance. The results are presented as the mean and the standard deviation. (C) HepG2 cells were grown under normal (4.5g/l glucose) culture conditions (Control) or were glucose starved for 5 h, and then restimulated with glucose-containing medium (4.5g/l) for 1 h before fixation and immunostaining for total and K8 pS74. Bars, 20 µm.

(5% milk in PBS and 0.1% Tween 20) and incubated with the designated antibodies. Nondenaturing gel electrophoresis was performed using the NativePAGE Bis-Tris gel system (Invitrogen) following the manufacturer's protocol. High salt extracts were performed using an established procedure (Ku et al., 2004).

AU gel electrophoresis

The AU gel method was adopted from a published protocol (Shechter et al., 2007). Upon solubilization of cells in NP-40 buffer, the insoluble pellets were dissolved by vortexing and homogenization in an appropriate volume of AU sample buffer (0.36 g urea, 100 µl of 0.2% Pyronin Y, 50 µl glacial acetic acid, and 500 µl of 25mg/ml protamine sulfate) and separated on 8% AU gels. Each 8% AU mini-gel was prepared by mixing 3.6 g urea, 1.3 ml acrylamide/bis-acrylamide (60:0.4), 0.5 ml of acetic acid, 4.4 ml of water, 60 µl TEMED, and 140 µl of ammonium persulfate (10%). The gels were run at 200 V in 5% acetic acid (running buffer) for 60–90 min, and then transferred onto PVDF membranes (25 min, 500 mA) in 0.7% acetic acid (transfer buffer) followed by Coomassie blue staining or immunoblotting.

Immunofluorescence staining and confocal imaging

The cells were fixed in methanol for 10 min at −20°C, air dried for 15 min, and incubated in blocking solution (PBS/2.5% wt/vol BSA/2% goat serum). Primary antibodies were added for 1 h, followed by three PBS washes and incubation with Alexa Fluor–conjugated secondary antibodies for 30 min. All incubations were performed at room temperature. After overnight mounting in ProLong Gold containing DAPI (Invitrogen), the cells were imaged on a laser-scanning confocal microscope (FluoView 500; Olympus) using a 60× oil immersion (1.4 NA) objective. Images were magnified using FluoView software (version 5.0; Olympus). An 405-nm laser diode, 488-nm argon laser, and 543-nm HeNe green laser were used to excite DAPI, Alexa Fluor 488, and Alexa Fluor 594, respectively. Signal separation was maximized by sequential scanning.

Human and animal liver experiments

Human liver tissues were used under an approved human subjects protocol. Non-diseased and diabetic human liver tissues were obtained from the National Disease Research Interchange. Cirrhotic liver explants were obtained from patients who underwent liver transplantation for end-stage liver disease (Ku et al., 2005). Animal use was approved by, and performed in accordance with, the University Committee on Use and Care of Animals at the University of Michigan. Livers were isolated from four different male 8-wk-old human K8-overexpressing transgenic mice (FVB/N background) for mass spectrometry analysis (performed by MS Bioworks) of human K8 acetylation sites. For the mass spectrometry analysis, K8 was enriched by high salt extraction followed by SDS-PAGE electrophoresis and excision of the protein band. Livers from female 12-wk-old leptin-deficient ob/ob mice and corresponding age- and sex-matched WT C57BL/6J mice were used to assess K8 acetylation under hyperglycemic and normoglycemic conditions (three mice/group). The total body weights for the WT and ob/ob mice, respectively, were 18.7 ± 0.3 and 42.7 ± 1.3 g ($P < 0.0001$), with corresponding blood glucose values of 230 ± 22 and 535 ± 84 mg/dl ($P = 0.02$).

Data analysis

The graph data were presented and statistically analyzed using Prism 5 software (GraphPad Software). Photoshop (CS2; Adobe) was used for immunoblot densitometry (Fig. 2, D and E; Fig. 5 B; and Fig. S3 A). National Institutes of Health ImageJ software was used to create the signal intensity plots shown in Fig. 2 B (raw data numbers plotted) by drawing 10-µm-long lines originating from the nuclei and performing a plot profile analysis, which provides the signal intensity as a function distance (as shown in Fig. S2).

Online supplemental material

Fig. S1 supports the data presented in Figs. 1 and 2 and shows the lysine residues selected for the analysis based on mass spectrometry data, conservation of the major K8 acetylation site (Lys-207) in all IFs (Type I–VI), and immunoblots of K8 and its acetylation site mutants. Fig. S2 supports data presented in Fig. 2 (A and B) and shows additional examples of filament organization of WT K8 and its acetylation-site mutants and an example of signal intensity measurement for perinuclear K8 filaments. Fig. S3 supports the data presented in Figs. 3 and 4 and shows quantification of the K8 AcK signal in WT and ob/ob mouse livers and corresponding SIRT2 levels and keratin filament organization; SIRT2 expression and acetylation of K8 in cirrhotic human livers; immunostaining for AcK and K8 upon SIRT2 knockdown; and Coomassie stain and K18 blot upon pharmacologic SIRT2 inhibition. Online supplemental material is available at http://www.jcb.org/cgi/content/full/jcb.201209028/DC1.

This work was supported by National Institutes of Health grants R01 DK52951 (M.B. Omary), K01 DK093776 (N.T. Snider), and P30 DK34933 (University of Michigan).

Submitted: 6 September 2012
Accepted: 29 December 2012

References

Aka, J.A., G.W. Kim, and X.J. Yang. 2011. K-acetylation and its enzymes: overview and new developments. *Handb Exp Pharmacol.* 206:1–12. http://dx.doi.org/10.1007/978-3-642-21631-2_1

Choudhary, C., C. Kumar, F. Gnad, M.L. Nielsen, M. Rehman, T.C. Walther, J.V. Olsen, and M. Mann. 2009. Lysine acetylation targets protein complexes and co-regulates major cellular functions. *Science.* 325:834–840. http://dx.doi.org/10.1126/science.1175371

Dryden, S.C., F.A. Nahhas, J.E. Nowak, A.S. Goustin, and M.A. Tainsky. 2003. Role for human SIRT2 NAD-dependent deacetylase activity in control of mitotic exit in the cell cycle. *Mol. Cell. Biol.* 23:3173–3185. http://dx.doi.org/10.1128/MCB.23.9.3173-3185.2003

Hasmann, M., and I. Schemainda. 2003. FK866, a highly specific noncompetitive inhibitor of nicotinamide phosphoribosyltransferase, represents a novel mechanism for induction of tumor cell apoptosis. *Cancer Res.* 63:7436–7442.

Herrmann, H., S.V. Strelkov, P. Burkhard, and U. Aebi. 2009. Intermediate filaments: primary determinants of cell architecture and plasticity. *J. Clin. Invest.* 119:1772–1783. http://dx.doi.org/10.1172/JCI38214

Imai, S., and L. Guarente. 2010. Ten years of NAD-dependent SIR2 family deacetylases: implications for metabolic diseases. *Trends Pharmacol. Sci.* 31:212–220. http://dx.doi.org/10.1016/j.tips.2010.02.003

Janke, C., and J.C. Bulinski. 2011. Post-translational regulation of the microtubule cytoskeleton: mechanisms and functions. *Nat. Rev. Mol. Cell Biol.* 12:773–786. http://dx.doi.org/10.1038/nrm3227

Kim, G.W., and X.J. Yang. 2011. Comprehensive lysine acetylomes emerging from bacteria to humans. *Trends Biochem. Sci.* 36:211–220. http://dx.doi.org/10.1016/j.tibs.2010.10.001

Kim, S.C., R. Sprung, Y. Chen, Y. Xu, H. Ball, J. Pei, T. Cheng, Y. Kho, H. Xiao, L. Xiao, et al. 2006. Substrate and functional diversity of lysine acetylation revealed by a proteomics survey. *Mol. Cell*. 23:607–618. http://dx.doi.org/10.1016/j.molcel.2006.06.026

Kim, H.S., A. Vassilopoulos, R.H. Wang, T. Lahusen, Z. Xiao, X. Xu, C. Li, T.D. Veenstra, B. Li, H. Yu, et al. 2011. SIRT2 maintains genome integrity and suppresses tumorigenesis through regulating APC/C activity. *Cancer Cell*. 20:487–499. http://dx.doi.org/10.1016/j.ccr.2011.09.004

Krishnan, J., C. Danzer, T. Simka, J. Ukropec, K.M. Walter, S. Kumpf, P. Mirtschink, B. Ukropcova, D. Gasperikova, T. Pedrazzini, and W. Krek. 2012. Dietary obesity-associated Hif1α activation in adipocytes restricts fatty acid oxidation and energy expenditure via suppression of the Sirt2-NAD+ system. *Genes Dev.* 26:259–270. http://dx.doi.org/10.1101/gad.180406.111

Ku, N.O., and M.B. Omary. 1997. Phosphorylation of human keratin 8 in vivo at conserved head domain serine 23 and at epidermal growth factor-stimulated tail domain serine 431. *J. Biol. Chem.* 272:7556–7564.

Ku, N.O., S. Azhar, and M.B. Omary. 2002. Keratin 8 phosphorylation by p38 kinase regulates cellular keratin filament reorganization: modulation by a keratin 1-like disease causing mutation. *J. Biol. Chem.* 277:10775–10782. http://dx.doi.org/10.1074/jbc.M107623200

Ku, N.O., D.M. Toivola, Q. Zhou, G.Z. Tao, B. Zhong, and M.B. Omary. 2004. Studying simple epithelial keratins in cells and tissues. *Methods Cell Biol.* 78:489–517. http://dx.doi.org/10.1016/S0091-679X(04)78017-6

Ku, N.O., J.K. Lim, S.M. Krams, C.O. Esquivel, E.B. Keeffe, T.L. Wright, D.A. Parry, and M.B. Omary. 2005. Keratins as susceptibility genes for end-stage liver disease. *Gastroenterology*. 129:885–893. http://dx.doi.org/10.1053/j.gastro.2005.06.065

Kwan, R., S. Hanada, M. Harada, P. Strnad, D.H. Li, and M.B. Omary. 2012. Keratin 8 phosphorylation regulates its transamidation and hepatocyte Mallory-Denk body formation. *FASEB J.* 26:2318–2326. http://dx.doi.org/10.1096/fj.11-198580

L'Hernault, S.W., and J.L. Rosenbaum. 1985. *Chlamydomonas* alpha-tubulin is posttranslationally modified by acetylation on the epsilon-amino group of a lysine. *Biochemistry.* 24:473–478. http://dx.doi.org/10.1021/bi00323a034

Leech, S.H., C.A. Evans, L. Shaw, C.H. Wong, J. Connolly, J.R. Griffiths, A.D. Whetton, and B.M. Corfe. 2008. Proteomic analyses of intermediate filaments reveals cytokeratin8 is highly acetylated—implications for colorectal epithelial homeostasis. *Proteomics*. 8:279–288. http://dx.doi.org/10.1002/pmic.200700404

Liao, J., N.O. Ku, and M.B. Omary. 1997. Stress, apoptosis, and mitosis induce phosphorylation of human keratin 8 at Ser-73 in tissues and cultured cells. *J. Biol. Chem.* 272:17565–17573. http://dx.doi.org/10.1074/jbc.272.28.17565

Loranger, A., S. Duclos, A. Grenier, J. Price, M. Wilson-Heiner, H. Baribault, and N. Marceau. 1997. Simple epithelium keratins are required for maintenance of hepatocyte integrity. *Am. J. Pathol.* 151:1673–1683.

Nakamichi, I., D.M. Toivola, P. Strnad, S.A. Michie, R.G. Oshima, H. Baribault, and M.B. Omary. 2005. Keratin 8 overexpression promotes mouse Mallory body formation. *J. Cell Biol.* 171:931–937. http://dx.doi.org/10.1083/jcb.200507093

Omary, M.B., N.O. Ku, J. Liao, and D. Price. 1998. Keratin modifications and solubility properties in epithelial cells and in vitro. *Subcell. Biochem.* 31:105–140.

Omary, M.B., N.O. Ku, G.Z. Tao, D.M. Toivola, and J. Liao. 2006. "Heads and tails" of intermediate filament phosphorylation: multiple sites and functional insights. *Trends Biochem. Sci.* 31:383–394. http://dx.doi.org/10.1016/j.tibs.2006.05.008

Omary, M.B., N.O. Ku, P. Strnad, and S. Hanada. 2009. Toward unraveling the complexity of simple epithelial keratins in human disease. *J. Clin. Invest.* 119:1794–1805. http://dx.doi.org/10.1172/JCI37762

Outeiro, T.F., E. Kontopoulos, S.M. Altmann, I. Kufareva, K.E. Strathearn, A.M. Amore, C.B. Volk, M.M. Maxwell, J.C. Rochet, P.J. McLean, et al. 2007. Sirtuin 2 inhibitors rescue alpha-synuclein-mediated toxicity in models of Parkinson's disease. *Science*. 317:516–519. http://dx.doi.org/10.1126/science.1143780

Schwer, B., and E. Verdin. 2008. Conserved metabolic regulatory functions of sirtuins. *Cell Metab.* 7:104–112. http://dx.doi.org/10.1016/j.cmet.2007.11.006

Shechter, D., H.L. Dormann, C.D. Allis, and S.B. Hake. 2007. Extraction, purification and analysis of histones. *Nat. Protoc.* 2:1445–1457. http://dx.doi.org/10.1038/nprot.2007.202

Snider, N.T., S.V. Weerasinghe, J.A. Iñiguez-Lluhí, H. Herrmann, and M.B. Omary. 2011. Keratin hypersumoylation alters filament dynamics and is a marker for human liver disease and keratin mutation. *J. Biol. Chem.* 286:2273–2284. http://dx.doi.org/10.1074/jbc.M110.171314

Strnad, P., Q. Zhou, S. Hanada, L.C. Lazzeroni, B.H. Zhong, P. So, T.J. Davern, W.M. Lee, and M.B. Omary; Acute Liver Failure Study Group. 2010. Keratin variants predispose to acute liver failure and adverse outcome: race and ethnic associations. *Gastroenterology.* 139:828–835: 835: e1–e3. http://dx.doi.org/10.1053/j.gastro.2010.06.007

Toivola, D.M., P. Strnad, A. Habtezion, and M.B. Omary. 2010. Intermediate filaments take the heat as stress proteins. *Trends Cell Biol.* 20:79–91. http://dx.doi.org/10.1016/j.tcb.2009.11.004

Yang, X.J., and E. Seto. 2008. Lysine acetylation: codified crosstalk with other posttranslational modifications. *Mol. Cell*. 31:449–461. http://dx.doi.org/10.1016/j.molcel.2008.07.002

Zhao, S., W. Xu, W. Jiang, W. Yu, Y. Lin, T. Zhang, J. Yao, L. Zhou, Y. Zeng, H. Li, et al. 2010. Regulation of cellular metabolism by protein lysine acetylation. *Science*. 327:1000–1004. http://dx.doi.org/10.1126/science.1179689